ELSEVIER

Journal of Volcanology and Geothermal Research 79 (1997) 149–168

Journal of volcanology and geothermal research

Structural settings of hydrothermal outflow: Fracture permeability maintained by fault propagation and interaction

Daniel Curewitz *, Jeffrey A. Karson

Department of Geology, Duke University, Durham, NC 27708-90229, USA

Received 6 April 1996; accepted 4 June 1997

Abstract

Hydrothermal outflow occurs most commonly at the terminations of individual faults and where multiple faults interact. These areas of fault propagation and interaction are sites of elevated stress termed breakdown regions. Here, stress concentrations cause active fracturing and continual re-opening of fluid-flow conduits, permitting long-lived hydrothermal flow despite potential clogging of fractures due to mineral precipitation. As fault systems evolve, propagation, interaction, and linkage of fault segments result in the migration and eventual localization of breakdown regions in kinematically favorable sites such as fault bends or fault intersections. Concurrent migration of hydrothermal outflow sites along with these areas of elevated permeability leads to predictable patterns of hydrothermal deposition along fault zones. Thus, the distribution of active outflow sites and preserved deposits along fault zones can potentially provide a tool for studying fault-zone evolution. © 1997 Elsevier Science B.V.

Keywords: hydrothermal activity; hot springs; fault propagation; fault tips

1. Introduction

It is clear that faults and fractures play a major role in the localization and evolution of hydrothermal flow on several scales (Norton and Knapp, 1977; Kerrich, 1986; Henley and Adams, 1992; Arribas, 1995). This follows from the nearly ubiquitous close association of faults and active hydrothermal outflow sites (including hot springs, geysers, fumaroles, submarine black- and white-smoker vents, mud volcanoes and other forms of hot seeps and flows, hereafter referred to collectively as 'hot springs'). Similar evidence for fault control of hydrothermal activity is reflected in the association between faults, ore deposits, and other centers of hydrothermal alteration (Kerrich, 1986).

Hydrothermal activity is dependent upon the interaction between a heat source, circulating fluids, and permeable pathways. Heat sources for hydrothermal systems include young dikes and plutons (Elders et al., 1984; Henley and Brown, 1985; Wohletz and Heiken, 1992; Embley and Chadwick, 1994; Embley et al., 1995), elevated geotherms due to tectonic activity (McKenzie, 1978; Henley and Brown, 1985), and frictional heating due to fault slip (Lachenbruch, 1980; Scholz, 1980). Circulating hydrothermal fluids include seawater (Mottl, 1983), meteoric groundwater, connate water (Henley and Brown, 1985; Carter

* Corresponding author.

PII S0377-0273(97)00027-9

et al., 1990) and juvenile-magmatic or deep crustal fluids (Kerrich, 1986; Carter et al., 1990; Kelley et al., 1993).

The elevated permeability required for observed rates of hydrothermal outflow must be related to high fracture density, because non-fractured rock has intrinsically low bulk permeability, typically 10^{-4}–10^{-17} darcy in crystalline rock and 10^{-2}–10^{-11} darcy in sedimentary rocks (Norton and Knapp, 1977; Brace, 1980). Permeability in fractured rock is much higher, with in situ values of 10^{1}–10^{-3} darcy (Brace, 1980). Fine-scale fracturing is closely related to faulting, as is clear from studies of fault zones showing that micro- and macrofracture density increase significantly (by at least an order of magnitude) near faults (Anders and Wiltschko, 1994).

Hydrothermal mineral precipitation is very efficient at filling fractures and void spaces. Significant mineral precipitation may occur over hundreds of years (Rimstidt and Barnes, 1980; Fournier, 1989), and would be expected to decrease permeability in fractures, thus inhibiting fluid circulation (Elders et al., 1979, 1984; Sibson, 1987). However, estimates of fluid flux based on water/rock ratios in both active and fossil hydrothermal systems suggest that high permeability and fluid circulation can be long-lived (Mottl, 1983; Kerrich, 1986; Barton et al., 1995). This is supported by radiometric dates from hydrothermal deposits that suggest continued hydrothermal activity over thousands to tens of thousands of years (Fournier, 1989; Lalou et al., 1993). Continued hydrothermal circulation despite rapid mineral precipitation in permeable pathways can be maintained by the active fracturing that results in new or rejuvenated conduits for fluid flow.

In order to investigate the connection between faults, fractures, and hot spring locations, we used published data to map the locations of hot springs with respect to known fault structures in 25 sites worldwide. These locations are then interpreted on the basis of different permeability maintenance mechanisms that we infer from fault geometry and kinematics. These results are highlighted in several examples from different hydrothermal fields around the world. We use these data to construct a qualitative model for the evolution of hydrothermal systems and fault zones.

2. Structural settings of hot springs

Published maps of hydrothermal fields in four different tectonic settings (mid-ocean ridges, volcanic arcs, continental rifts and hot spots) are used to explore the spatial relationships between faults and hydrothermal flow. Several locales within each tectonic setting (Table 1) spanning an areal range from < 0.5 to > 50 km^2 are investigated. Fault maps, geologic maps, and geothermal resource maps, commonly from different sources and made using different mapping techniques, were combined to show the locations of hot springs relative to local geologic and structural features.

Analyzing these data involves making assumptions about fault-scaling relationships, fracture-network geometry, and mechanical behavior of different rock-types under different loading conditions. Comparison of data across these scales is possible because fault parameters such as the displacement–length ratio (Peacock, 1991; Scholz et al., 1993; Peacock and Sanderson, 1994), or the scarp area–fault length ratio (Dawers et al., 1993) are considered scale independent. Additionally, field and laboratory measurements suggest no significant difference in fault system or fracture set geometry, regardless of scale, rock type, tectonic environment, or loading conditions (Aydin and Reches, 1982; Sibson, 1987; Cowie and Scholz, 1992).

2.1. High-permeability sites along faults

Based on recurring patterns, hot springs along fault zones are catalogued in terms of five specific structural settings, described in more detail below: (1) fault terminations or 'tip-line areas'; (2) fault overlaps or 'interaction areas'; (3) 'locked' fault-intersection areas; (4) 'slipping' fault-intersections; and (5) fault traces (Fig. 1). Some of the hot springs are not near any mapped faults, and we refer to these hot springs as 'asystematic' with respect to known faults. In some of these locations it is possible that faults and fracture systems are covered by surficial deposits. Alternatively, high-permeability conduits for fluid flow may be provided by exposed aquifers and bedding surfaces (Person et al., 1996), or igneous contacts such as dike and pluton margins (Martel and Petersen, 1991; Boullier et al., 1994).

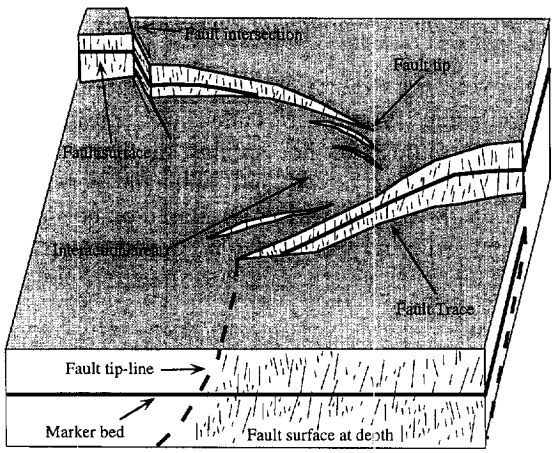

Fig. 1. Schematic diagram showing different geometric and kinematic characteristics of a fault zone. Fine lines on the fault surfaces represent slickenlines, and the bold line is a marker bed to show displacement across the faults.

2.1.1. Fault tip-lines

Faults typically have displacement gradients from maximum slip near the center to zero at the fault terminations, defined as fault tips (Boyer and Elliott, 1982). In three dimensions, a fault termination is defined by a curvilinear trace called the fault tip-line. Stresses associated with the displacement gradient are concentrated at tip lines, and drive crack propagation into non-fractured rock. The area of intense fracturing around the fault tip-line is called the 'breakdown region' (Fig. 2A; Scholz et al., 1993), the dimensions of which are proportional to fault length. Specifically the radius of the breakdown region is equal to 5 to 10% of the length of the fault (Cowie and Scholz, 1992; Scholz et al., 1993). We refer to hot springs within the breakdown region of a fault tip as 'tip-line hot springs'.

2.1.2. Fault interaction areas

Where two or more fault tip-lines are in close proximity, the individual breakdown regions merge, forming a single, modified breakdown region where stresses associated with the two fault tips interact. The size and shape of this resulting breakdown region is controlled by the specific geometry and kinematics of the individual faults (Du and Aydin, 1995). In the simple case of two overlapping faults, the size and shape of the breakdown region is defined by fault lengths, fault spacing, the amount of overlap, and fault kinematics (Fig. 2B). We use stress concentrations derived for different geometric and kinematic configurations depicted in published reports (Segall and Pollard, 1980; Aydin and Page,

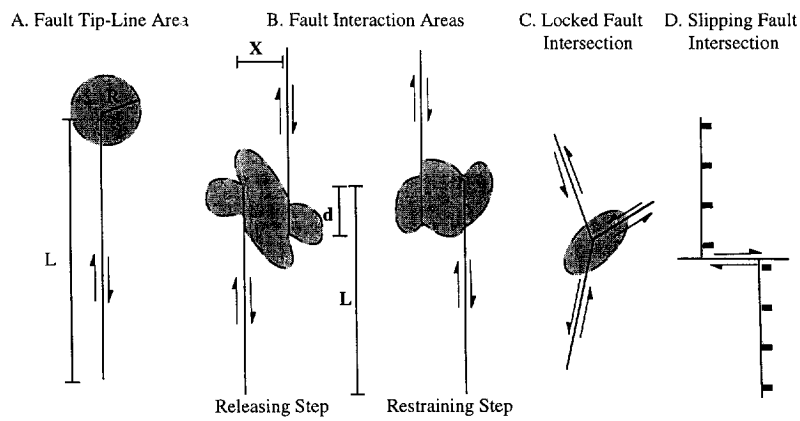

Fig. 2. Schematic diagrams showing 'breakdown' regions of concentrated stress (surrounded by dashed lines) associated with different fault geometries. (A) The radius (R) of the breakdown region (gray area) around the termination of an isolated fault is proportional to 0.1 L, where L is the half-length of the fault (after Pollard and Aydin, 1988; Scholz et al., 1993). (B) Different shapes and sizes of the breakdown region are found in areas with different fault geometry and kinematics. In this case the diagram shows two types strike-slip fault interactions: a releasing step with focused tensile stresses and a dilational step with focused compressional stresses (Isida, 1976; Segall and Pollard, 1980; Aydin and Page, 1984; Burgmann and Pollard, 1994). (C) Some fault intersections will be locked, with areas of high stress concentrations (shown schematically) near the intersection (e.g., Andrews, 1989). (D) Faults with the same slip lines intersect at 'slipping fault-intersections' with stresses determined by friction on the faults (e.g. Bruhn et al., 1990).

1984) to estimate the size and shape of the theoretical breakdown region between interacting faults. We refer to hot springs that occur within these areas as 'interaction-area hot springs'.

2.1.3. Fault intersections

The junction of two or more faults can behave in a variety of ways depending on fault geometry and kinematics. Locked fault-intersections (Fig. 2C) occur where the slip vectors of intersecting faults have non-parallel or even opposing directions. This kinematic incompatibility typically results in one fault that transects and displaces the other faults, which are abandoned or locked (Andrews, 1989). Opposing slip vectors and associated kinematic incompatibilities give rise to a breakdown region in the fault intersection area. 'Locked-intersection hot springs' are found at the junction of faults with converging slip directions, such as conjugate strike-slip faults.

Where the slip vectors on intersecting faults are parallel, no kinematic incompatibility develops at the point of intersection (Fig. 2D; Andrews, 1989; Bruhn et al., 1990). We refer to these areas as 'slipping fault-intersections', and expect that no significant breakdown region will form, as little stress buildup or active fracturing is likely to occur away from the fault-intersection area. 'Slipping-intersection hot springs' are found at the junction of faults with parallel slip vectors, such as transfer faults along extensional fault systems or intersecting vertical-slip faults.

2.1.4. Fault traces

The intersection of a fault plane with the earth's surface, a fault trace, commonly marks the topographic expression of an active fault or deep levels of an inactive fault exposed by erosion. Localized fracturing due to friction on the fault during slip, or asperity crushing due to interaction of irregular fault surfaces can form highly fractured volumes of rock along a fault zone. Long-term fault slip can give rise to anisotropic permeability as bands of fault gouge and cataclasite develop parallel to the fault surface (Scholz and Anders, 1994). These different mechanisms may form and maintain fracture permeability along fault surfaces and can act to channel hydrothermal fluids into springs we refer to as 'fault trace hot springs'.

2.2. Permeability maintenance mechanisms

In order to explore further the relationship of hydrothermal systems to faults, we consider the structural settings of hot springs in terms of the mechanisms that create and maintain permeable pathways for fluid flow (Fig. 3). Based on hot spring locations with respect to faults, we interpret hy-

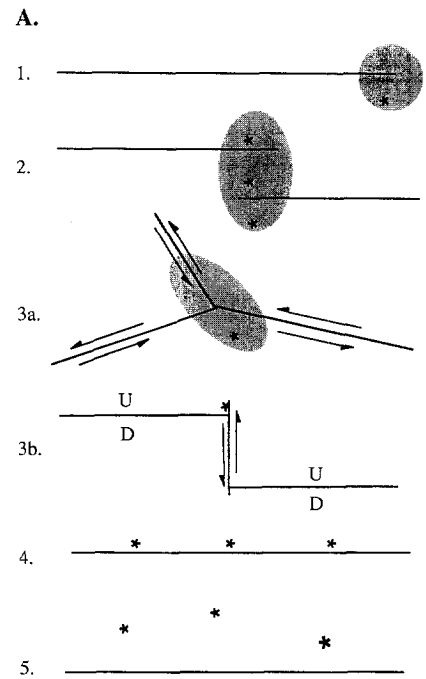

B.

Structural Settings	Mechanical Interpretation
1. Tip-line Area	Dynamically Maintained
2. Fault Interaction Area	
3a. Locked Fault-Intersection	
3b. Slipping Fault-Intersection	Kinematically Maintained
4. Fault Trace	
5. Asystematic	

Fig. 3. (A) Schematic diagram showing examples of the different structural settings of hydrothermal vents (★) relative to faults (straight lines). Breakdown regions are shaded. (B) Table summarizing the structural settings of hot springs and corresponding mechanical interpretations of hot spring locations. See text for explanation and discussion.

drothermal outflow areas in terms of two primary mechanisms of forming and sustaining fracture permeability in the crust. In the first case, fault propagation or interaction in tip-line areas, fault interaction areas, and locked fault intersections leads to stress concentration and fracturing away from the main fault. These fracture systems correspond to the breakdown regions described above, and we refer to them as 'dynamically maintained fracture systems'. Alternatively, slip along fault traces or at slipping fault-intersections can re-open pre-existing fracture networks along a fault. In these areas, fracturing is limited to the immediate vicinity of the fault. We refer to these types of fracture networks as 'kinematically maintained fracture systems'.

2.2.1. Dynamically maintained fracture systems

Relatively high stresses are required to fracture fresh rock, and it is generally accepted that these stresses are achieved by stress concentration at the tips of faults and fractures (Scholz, 1990; Cowie and Scholz, 1992). Microearthquake swarms (Sibson, 1985, 1987), aftershock concentrations (Scholz, 1990; King et al., 1994; Stein et al., 1995), and arrays of micro-faults and fractures (Peacock and Sanderson, 1995) are interpreted as evidence for stress concentration in these areas. Fracture arrays with distinctive Mode I (opening), Mode II (shearing, slip normal to the crack tip), and Mode III (shearing, slip parallel to the crack tip) geometries form at mechanically predictable angles to the main fault, given the slip direction and fault geometry (Fig. 4; Allmendinger et al., 1989; Scholz et al., 1993; Peacock and Sanderson, 1995). Most relevant to the present study is the formation of extension, or Mode I fractures, which can provide high permeability fluid-flow conduits. Maintenance of these permeable pathways in the breakdown region is dependent upon continued fault propagation or interaction, and we refer to hot springs found in these areas as 'dynamically maintained hot springs'.

2.2.2. Kinematically maintained fracture systems

As the breakdown region migrates with the fault tip-line, the newly formed fault zone will continue to slip in response to remote stresses. These stresses are generally much less than those required at tip lines for propagation. If fault propagation continues, the faults eventually join and form fault intersections or fault bends. Once this happens, the faults may become kinematically linked such that slip on any of them can influence the mechanical behavior of the others. Slip on any of an array of intersecting faults with common slip lines that do not offset or lock one another will tend to reactivate fractures at their intersection. Fracture permeability may be maintained by reopening of existing fracture systems due to fault slip, rather than the creation of new fractures in a breakdown region. Therefore, we refer to hot springs that occur in these areas as 'kinematically maintained hot springs'.

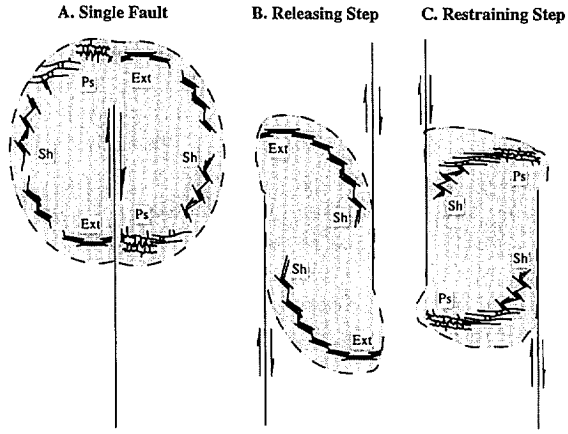

Fig. 4. Fractures expected to form within breakdown regions. (A) Schematic diagram summarizing the expected types of fractures and veins that might be found in different parts of the breakdown region around the tip of an isolated fault. (B) Diagram showing the types of fractures expected in a releasing step along a strike-slip fault zone. (C) Types of fractures expected in a restraining step along a strike-slip fault zone. Overprinting relationships between different fracture types are expected as two fault tips approach one another and interact. Mode I extension fractures (*Ext*) should form in areas of tensile stress, or in areas of mixed tensile and shear stress. Mode II and III shear fractures (*Sh*) should form in areas of transtension, transpression, or shear stress. Kink-bands, small thrust faults, folds, or pressure solution features (*Ps*) should accommodate shortening in areas of compression (modified after Segall and Pollard, 1980; Scholz et al., 1993; Burgmann and Pollard, 1994; Peacock and Sanderson, 1995).

3. Survey of active hydrothermal sites

In the following sections we outline a number of particularly well-documented examples of the rela-

tionship between active hot springs and faults, as well as between hot spring deposits and faults. These examples come from published reports, field investigations, or from combining fault and hydrothermal information from separate sources. These particular sites were chosen as representative of a variety of tectonic settings in order to emphasize the general applicability of our approach. We then present the results of a global survey of over 800 hot springs and statistics on the various types of occurrences with respect to both local structural settings and mechanical interpretation.

3.1. Examples of hot springs and associated faults

3.1.1. Endeavour hydrothermal field, Juan de Fuca Ridge, northeast Pacific Ocean

Delaney et al. (1992) combined submersible and high-resolution sonar mapping in order to survey of the Endeavour Hydrothermal Field on the northern Juan de Fuca Ridge, northeast Pacific Ocean (Fig. 5). The axial graben, where hydrothermal activity is centered, is lightly to moderately sedimented, with evidence of recent volcanic activity in the form of fresh lava tubes and pillows and a collapsed lava

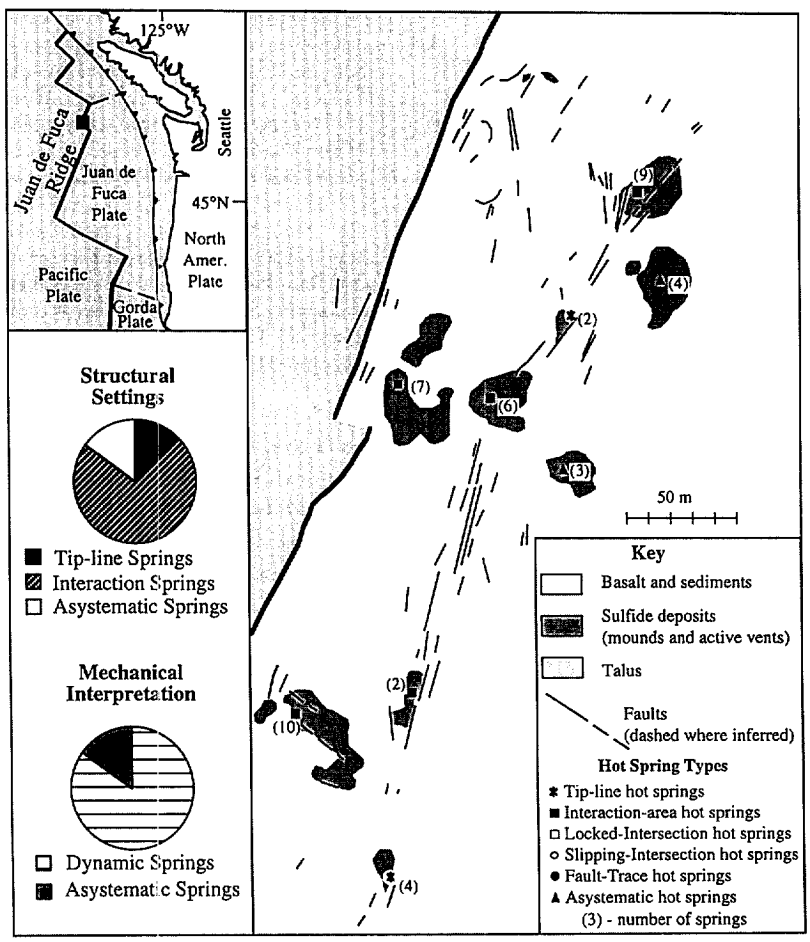

Fig. 5. Geologic map of the Endeavour Hydrothermal Field (after Delaney et al., 1992). Upper inset shows location on the Juan de Fuca Ridge in the northeast Pacific Ocean, lower inset shows pie charts of the proportions of hot springs in different structural settings and mechanical interpretations.

lake. Fault scarps generally trend N20°E and have relief on the order of 10–30 m. Fault surfaces and talus slopes are not sedimented, indicating that tectonic activity is recent or ongoing.

Hydrothermal activity occurs primarily as black smoker vents. Both active and inactive sulfide mounds are found at the tips of individual faults or where multiple fault tips overlap. Sulfide mounds commonly form where oblique fault trends converge, although actual fault intersections are rare. Offsets in the axial valley wall, interpreted as accommodation zones (a form of interaction area), are commonly the site of vigorous hydrothermal activity or large inactive sulfide mounds. The relative proportions of hot spring types found here are similar to other hydrothermal fields on the Juan de Fuca Ridge, and along other mid-ocean ridges (Table 1).

3.1.2. Southern Seismic Zone near Hengill, Iceland

Maps of seismically active normal faults (Foulger, 1988), and hot springs (Barth, 1950; Foulger, 1988) were used to investigate the southwestern region of Iceland near Hengill, an active rift zone near a hot spot (Fig. 6). Combining these two studies to make a compilation map of the Hengill area gives an excellent picture of local structural and hydrothermal features. The region is entirely covered by basaltic volcanic rocks related to mid-ocean ridge spreading and hot spot activity. Normal faults generally trend northeast, approximately perpendicular to the extension direction. Hydrothermal vents in this area are found primarily at the tips of faults and between overlapping fault tips. Despite their very different tectonic settings, the Hengill area of Iceland, at the Mid-Atlantic Ridge, and Yellowstone, a cratonic hot

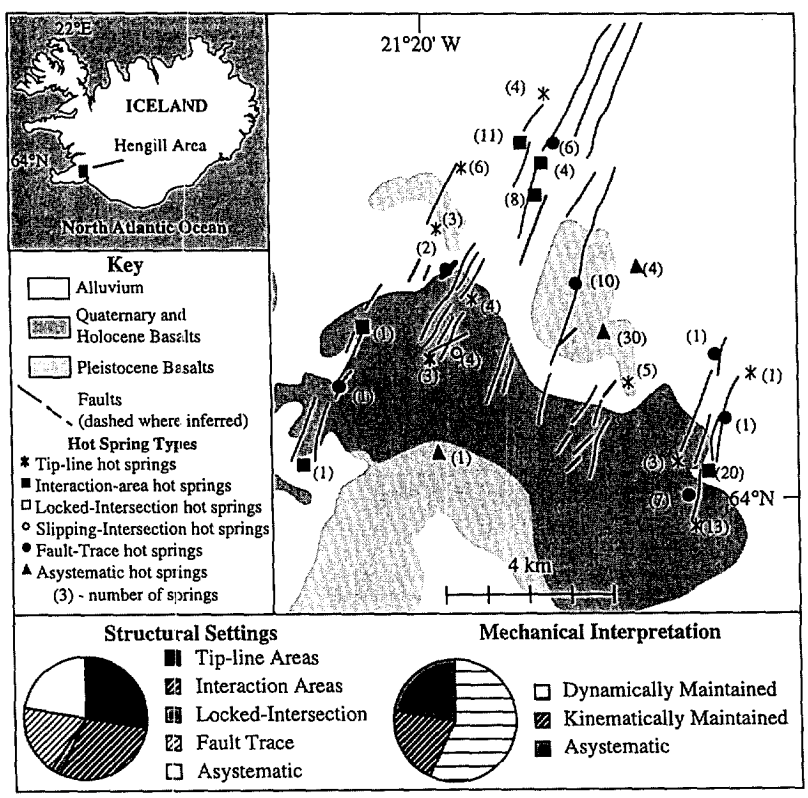

Fig. 6. Geologic map of the Hengill Area, Iceland (after Barth, 1950; Foulger, 1988). Upper inset shows location in Iceland, lower inset shows pie charts of the proportions of hot springs in different structural settings and mechanical interpretations.

Table 1
Number and percentage of hot springs catalogued by structural setting and then interpreted according to fault mechanics

Location	Structural settings										Mechanical interpretation				Asystematic		Total
	tip-line area		interaction area		locked fault-Int.		slipping fault-Int.		fault trace		dynamic		kinematic				
	(#)	(%)	(#)	(%)	(#)	(%)	(#)	(%)	(#)	(%)	(#)	(%)	(#)	(%)	(#)	(%)	
Mid-ocean ridge																	
Snake Pit (MAR 23°N) (1)	3	27	8	73	0	0	0	0	0	0	11	100	0	0	0	0	11
TAG (MAR 26°N) (2)	0	0	1	50	1	50	0	0	0	0	2	100	0	0	0	0	2
East Pacific Rise 10°N(3)	0	0	1	50	0	0	0	0	1	50	1	50	1	50	0	0	2
Gorda Ridge (NE Pacific 42°N) (4)	0	0	6	100	0	0	0	0	0	0	6	100	0	0	0	0	6
Juan de Fuca Ridge (47°57′N) (5, 6)	17	24	45	63	0	0	0	0	0	0	62	87	0	0	9	13	71
Total	20	22	61	66	1	1	0	0	1	1	82	89	1	1	9	10	92
Continental rift																	
Califomia (7)	13	52	0	0	3	12	1	4	4	16	16	64	5	20	4	16	25
Trans-Pecos Texas (8)	13	33	7	18	1	3	1	3	13	33	21	54	14	36	4	10	39
Utah, Nevada (9)	27	39	16	23	0	0	2	3	13	19	43	61	15	21	12	17	70
Tanzania (10, 11)	1	10	4	40	1	10	0	0	2	20	6	60	2	20	2	20	10
Kenya (12, 13, 14)	32	55	14	24	0	0	0	0	2	3	46	79	2	3	10	17	58
Menderes, Turkey (15)	5	19	5	19	2	7	0	0	11	41	12	44	11	41	4	15	27
Total	91	40	46	20	7	3	4	2	45	20	144	63	49	21	36	16	229
Magmatic arc																	
Japan (16, 17)	13	50	3	12	0	0	0	0	2	8	16	62	2	8	8	31	26
Caribbean (French Antilles) (18)	6	38	1	6	0	0	2	13	1	6	7	44	3	19	6	38	16
Columbia (19)	0	0	5	36	1	7	0	0	0	0	6	43	0	0	8	57	14
Mexico (20 21)	12	39	7	23	2	6	0	0	10	32	21	68	10	32	0	0	31
New Zealand (22, 23)	64	38	14	8	7	4	8	5	35	21	85	50	43	25	42	25	170
Total	95	37	30	12	10	4	10	4	48	19	135	53	58	23	64	25	257
Hot spot																	
Iceland (24, 25)	42	27	45	29	4	3	0	0	28	18	91	59	28	18	34	22	153
Yellowstone (26, 27)	16	18	29	32	0	0	0	0	5	5	45	49	5	5	41	45	91
Total	58	24	74	30	4	2	0	0	33	14	136	56	33	14	75	31	244
Combined Total	264	32	211	26	22	3	14	2	127	15	497	60	141	17	184	22	822

Sources: (1) Gente et al., 1991; (2) Karson and Rona, 1990; (3) McConachy, 1984; (4) Kappel and Franklin, 1989; (5) Delaney et al., 1992; (6) Robigou et al., 1993; (7) Anderson and Axtell, 1972; (8) Henry, 1979; (9) Hewitt et al., 1972; (10) Tiercelin et al., 1989; (11) Ebinger et al., 1993; (12) Tole, 1990; (13) Cioni et al., 1992; (14) Grimaud et al., 1994; (15) Ten-Dam and Khrebtov, 1970; (16) Sato, 1970; (17) Yamasaki, 1970; (18) Cormy, 1970; (19) Arango, 1970; (20) Banwell and Valle, 1970; (21) Puente and De La Pena, 1979; (22) N.Z. Bulletin, 1963; (23) Grindley, 1970; (24) Foulger, 1988; (25) Barth, 1950; (26) Allen and Day, 1935; (27) Link et al., 1992.

spot (Allen and Day, 1935; Link et al., 1992), have similar proportions of different types of hot springs (Table 1).

3.1.3. *Lake Bogoria, East African Rift, Kenya and Menderes Massif, Turkey*

Cioni et al. (1992) conducted a study of the thermal waters near Lake Bogoria, and Grimaud et al. (1994) completed a structural and geologic map of the Baringo–Bogoria half-graben in the Eastern Branch of the East African Rift in southern Kenya (Fig. 7). Miocene, Pliocene and Pleistocene lava flows cover PreCambrian basement. Rift-lake sediments and Quaternary alluvium fill the deeper fault-bounded basins. A major normal fault borders the lake on the east, forming the eastern boundary of the Baringo–Bogoria half-graben. The rocks west of the lake are cut by N–S-striking normal faults which dip toward the lake.

At Bogoria 92% of the hot springs are found in tip-line or interaction areas. The highest temperature hot springs are found in the interaction area where the border fault is segmented on the southeast side of the lake. Lower temperature springs are found in the tip-line areas of the smaller faults found on the west side of the lake. The lowest temperatures are found

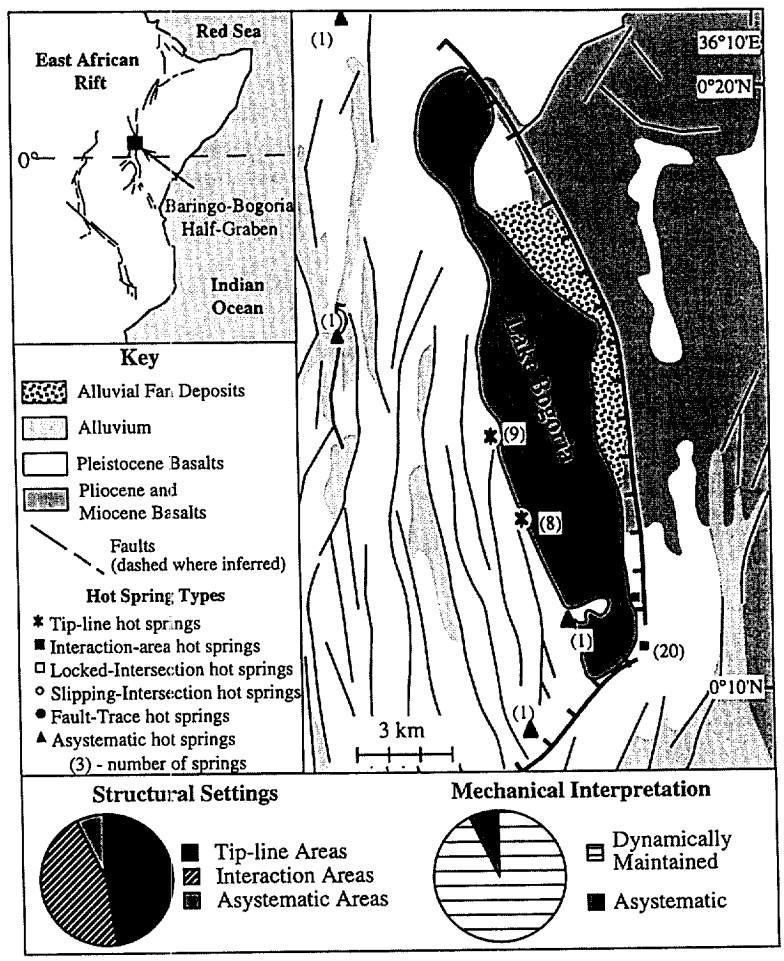

Fig. 7. Geologic map of the Lake Bogoria region, Kenya (after Cioni et al., 1992; Grimaud et al., 1994). Upper inset shows location in the East African Rift, lower inset shows pie charts of the proportions of hot springs in different structural settings and mechanical interpretations.

in asystematic hot springs farther out in the basin (Fig. 8A).

Comparison of hot spring locations and hydrothermal fluid temperatures from the Menderes Massif hydrothermal area, Turkey (Ten-Dam and Khrebtov, 1970) show a similar systematic relationship between hot spring type and hot spring temperature (Fig. 8B). In both of these areas, most hot springs are in dynamically maintained areas near fault tips and in interaction areas. The dynamically maintained hot springs exhibit significantly higher temperatures than the kinematically maintained hot springs. Asystematic hot springs are significantly cooler than both the kinematically and dynamically maintained hot springs.

3.1.4. Waiotapu Geothermal Field, New Zealand

The N. Z. Dep. Sci. Ind. Res. (1963) documents the geology and geothermal resources of the Waiotapu Geothermal Area on North Island (Fig. 9). The tectonics of the region are dominated by transform faulting and subduction of the Pacific and Australian plates along the Alpine Fault, Kermadec Trench, and Puysegur Thrust plate boundary system. The regional geology is dominated by a set of ENE-trending normal faults which dip to the northwest and cut a thick sequence of lavas and ignimbrites. The Waiotapu Fault's southern termination is at a fault splay characterized by several cross-cutting E–W- and N–S-trending normal faults. North of the present fault splay is an area of similar cross-cutting E–W- and N–S-trending faults, which may be a fossil fault splay.

Most hydrothermal activity in this area is concentrated at the termination of the large-scale Waiotapu fault zone that extends for several kilometers to the northeast of the mapped area. Hydrothermal vents are concentrated in tip-line and interaction areas of the smaller faults that comprise the fault splays in this area. This suggests that the regional distribution of hydrothermal activity may be controlled by large-scale fault geometry, while the smaller faults control the localization of hydrothermal outflow on the scale of this map.

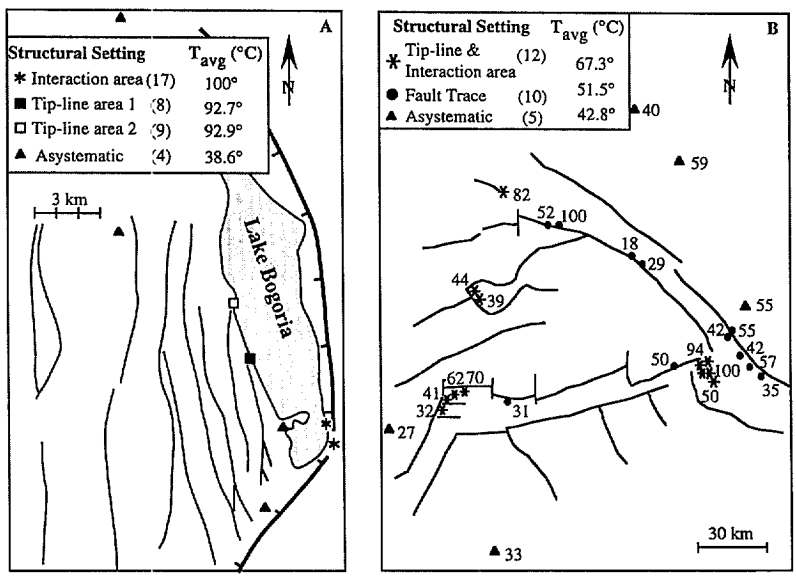

Fig. 8. (A) Simplified fault map of the Lake Bogoria, Kenya hydrothermal area showing the relationship between hot spring temperature and structural setting. Nearly all of the springs are dynamically maintained. Note that the hottest springs occur where the main border-fault (bold) changes strike. (B) Simplified fault map of the Menderes Massif, Turkey (after Ten-Dam and Khrebtov, 1970) showing a similar relationship between hot spring temperature and structural setting. The hottest springs are dynamically maintained, the coolest springs are asystematic, and the intermediate temperature springs are kinematically maintained. Temperature of each spring is shown in degrees Celsius.

3.1.5. Basin and Range, western US

Mapping of hydrothermal deposits and hot springs at Roosevelt Hot Springs KGRA (Known Geothermal Resource Area), UT (Fig. 10A) (after Sibbett and Nielson, 1980; Curewitz, unpubl. data) shows that the location of hot springs and the distribution and character of hot spring deposits are related to local faults. Several trends are clear from both the field work and map surveys of this area. First, most active hot springs are found at either fault tips or where multiple faults interact. Second, most hydrothermal deposits occur along faults. Hydrothermal deposits found at fault tips, fault intersections and in extensional duplexes (Fig. 10B) consist of relatively large volumes of opaline silica and quartz (for example $> 15{,}000$ m^3 at the southern tip of the Opal Mound Fault) deposited from hydrothermal fluids at temperatures greater than > 200°C (Elders et al., 1979; Hannington et al., 1995). In contrast, hot spring deposits along fault traces (Fig. 10C) occur as relatively low-volumes of calcite, clay, and amorphous silica (for example < 2500 m^3 along the trace of the Opal Mound Fault) deposited from hydrothermal fluids at temperatures less than 150°C (Elders et al., 1979).

Field work (Curewitz, unpubl. data) and map surveys of hydrothermal areas around the Basin and Range such as Steamboat Hot Springs KGRA, NV (White et al., 1964), and Coso Hot Springs KGRA, CA (Hulen, 1978) reveal similar relationships. Most

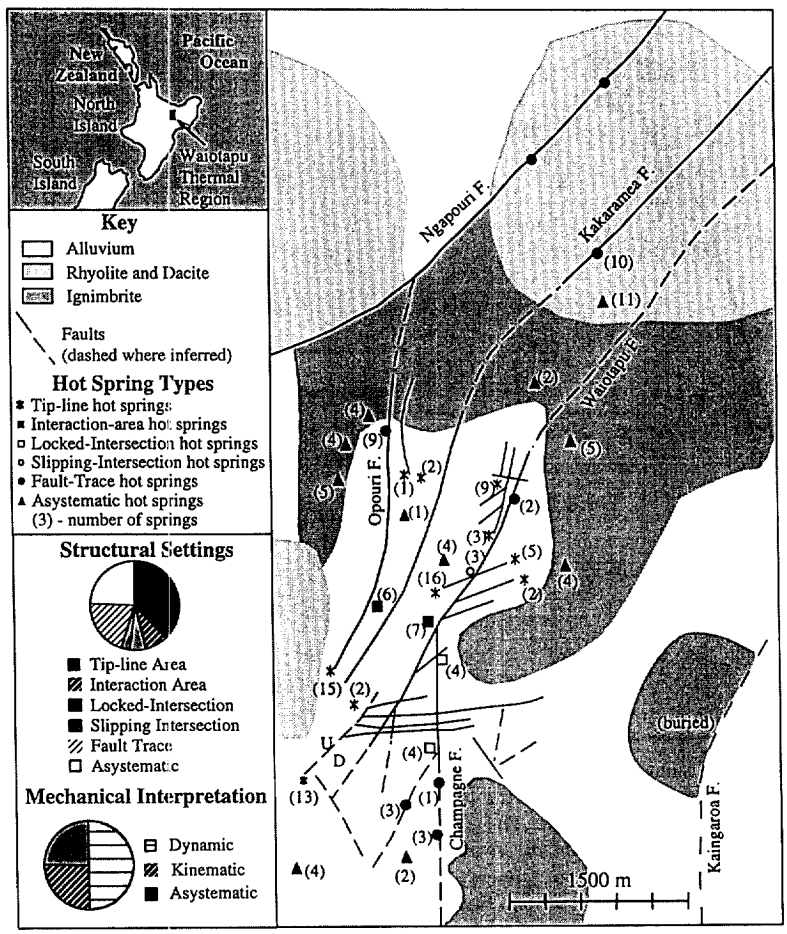

Fig. 9. Geologic map of the Waiotapu Geothermal field, North Island, New Zealand (from N. Z. Dep. Sci. Ind. Res., 1963). Upper inset shows location in the southeast Pacific, lower inset shows pie charts as in Fig. 5.

of the active hot springs in these areas are interpreted as 'dynamically maintained' based on their structural settings. Fault intersections, fault interaction areas and fault tip-lines host the bulk of the hydrothermal mineral deposits, which consist mainly of minerals precipitated from high-temperature fluids. Some fault traces are marked by thin (generally less than 1 m thick) veneers of hydrothermal minerals precipitated from relatively low-temperature fluids.

3.2. Global survey of hot springs

The results of our global survey of hot springs are recorded in Table 1, and summarized in Fig. 11.

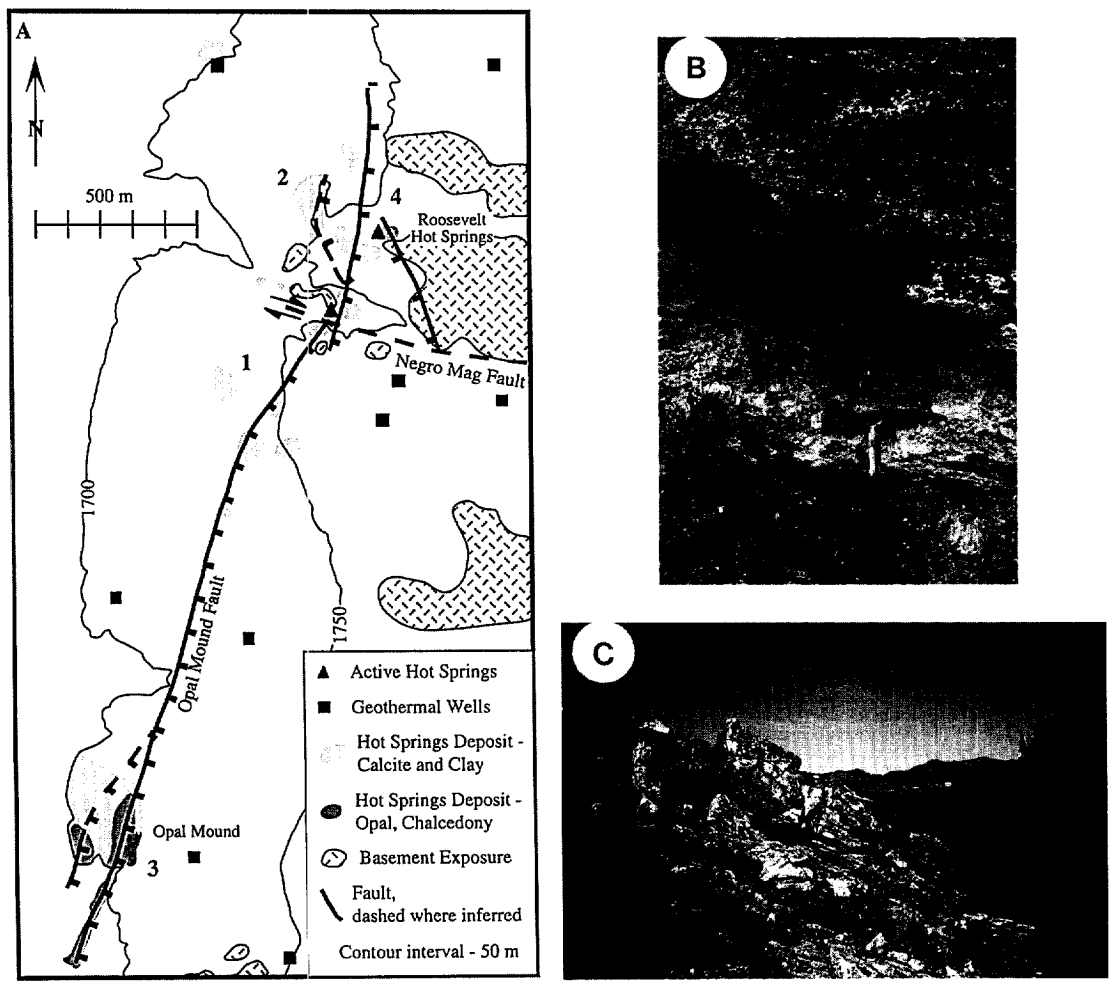

Fig. 10. (A) Map of Roosevelt Hot Springs KGRA, Beaver County, UT (after Sibbett and Nielson, 1980) showing the location of two active hot springs, both of which are dynamically maintained (tip-line hot spring and interaction area hot spring). Hot spring deposits are found along the Opal Mound Fault and the Negro Mag Fault. The most weathered deposits are found at *1*, and are covered by soil and vegetation; deposits at *2* are similar in appearance. At *3* (the Opal Mound), deposits are fresh looking with little or no soil cover or vegetation. At *4* (Roosevelt Hot Springs), deposits are fresh and are forming today due to active venting. (B) Photograph taken near *1* in (A) showing a hydrothermal deposit along the trace of the Opal Mound Fault. This deposit is highly weathered and consists mainly of calcite-cemented alluvium and clay, with some layers of amorphous silica. The deposit is elongate parallel to the fault, and has a maximum thickness of approximately 1 m. (C) Photograph showing a large hydrothermal deposit at the southern tip of the Opal Mound Fault, near *4* in (A). This deposit is fresh amorphous silica and opal, and forms an oval-shaped mound approximately 150 m across and up to 4 m tall at its center.

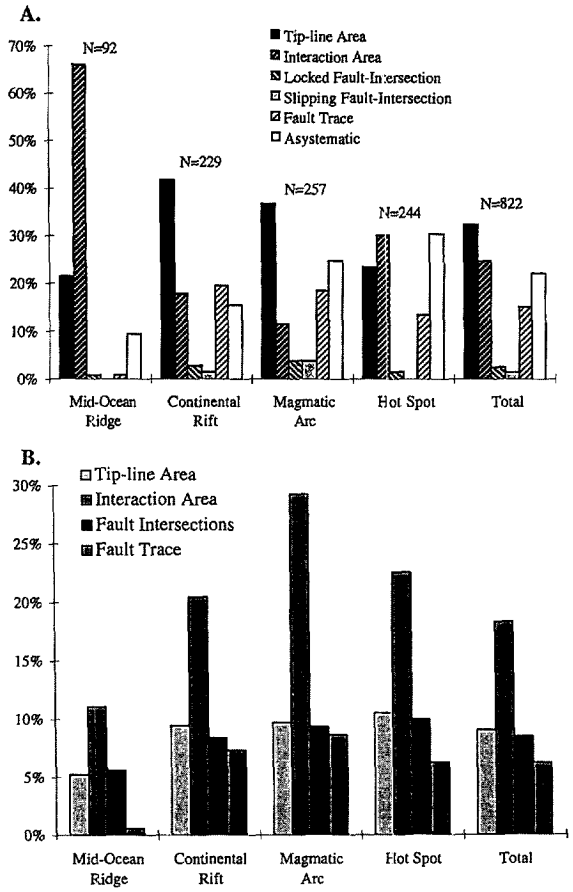

Fig. 11. (A) Relative proportions of hot springs in different structural settings. (B) Percentage of hydrothermally active sites normalized to the total abundance of each structural setting.

These results show that 78% of the hot springs are near faults, with only 22% found away from any mapped fault. The most common settings are fault tip-lines; hot springs in these areas comprise 33% of the 822 hot springs studied. Hot springs in interaction areas (25%) and fault traces (15%) are the next most common. Hot springs at locked fault-intersections (3%) and slipping fault-intersections (2%) are relatively rare (Fig. 11A).

Neglecting the 'asystematic' hot springs that are not associated with mapped faults (22%), the data show that the relative abundance of hot springs decreases from most common in tip-line areas to least common at fault intersections; generally hot springs at tip lines > interaction areas > fault traces ≫ locked fault-intersections > slipping fault-intersections. However, this distribution of hot springs does not hold for all the different tectonic settings; for example, mid-ocean ridges deviate from the overall data set, with 66% of the hot springs found in interaction areas. Deviations of up to 30% occur within a given structural setting between different tectonic environments (Fig. 11A; Table 1).

In order to evaluate the distribution of hot springs near faults, we normalized the number of hydrothermally active structural settings by the total number of occurrences of each site (Table 2). These results show that hydrothermal activity occurs in 18% of interaction areas, 11% of fault tip-lines, 9% of fault intersections, and only 6% of fault traces (Fig. 11B). While the absolute percentage of structural settings that host hydrothermal activity varies somewhat (by less than 7%) between different tectonic regimes, the trend from interaction areas > fault tip-lines > fault intersections > fault traces holds for each environment. We suggest that these results are an indication of the relative permeability of the different structural settings, and that the consistency of these data represent an underlying structural control of hydrothermal activity. Below we incorporate these data into a model for fault zone and hydrothermal system evolution.

4. Interpretation and discussion

4.1. Fault mechanics and permeability maintenance

As discussed in previous sections, we define two means of maintaining fracture-related permeability along faults: fracturing due to stress concentration (dynamic maintenance) and fracturing due to fault slip (kinematic maintenance). We interpret both the distribution of hot springs in different structural settings and the normalized distribution of hydrothermal activity (relative permeability) of these different structural settings in terms of these permeability maintenance mechanisms. In our interpretation dynamically maintained fracture systems (60% of the hot springs) are much more numerous than kinematically maintained fracture systems (17% of the hot springs) (Table 1; Fig. 12A). These proportions are consistent among different tectonic regimes and

Table 2
Total number of occurrences of each structural setting, number of hydrothermally active sites, and the normalized percentage of hydrothermally active sites in each tectonic regime

Location	Structural settings												Mechanical interpretation					
	tip-line area			interaction area			fault intersections (all)			fault trace			dynamically maintained			kinematically maintained		
	sites	active sites	percent	sites	active sites	percent	sites	active sites	percent	sites	active sites	percent	sites	actives ssites	percent	sites	active sites	percent
Mid-ocean ridge	153	8	5	135	15	11	18	1	6	170	1	1	288	23	8	305	2	1
Continental rift	402	38	9	127	26	20	119	10	8	521	38	7	529	64	12	648	48	7
Magmatic arc	257	25	10	41	12	29	64	6	9	173	15	9	298	37	12	214	21	10
Hot spot	180	19	11	62	14	23	10	1	10	176	11	6	242	33	14	238	12	5
Total	992	90	9	365	67	18	211	18	9	1040	65	6	1357	157	12	1405	83	6

References are the same as in Table 1.

among different locales within each regime. Additionally, the normalized data show the same trend, with a maximum of 8% variation (Table 2; Fig. 12B). This indicates that dynamically maintained fracture networks are more permeable and host a significantly higher proportion of the hot springs along a fault zone than kinematically maintained fracture networks. We infer that the formation and maintenance of permeable fracture systems, and hence the location of hot springs, is controlled by stress concentrations in breakdown regions that develop as a result of fault propagation and interaction.

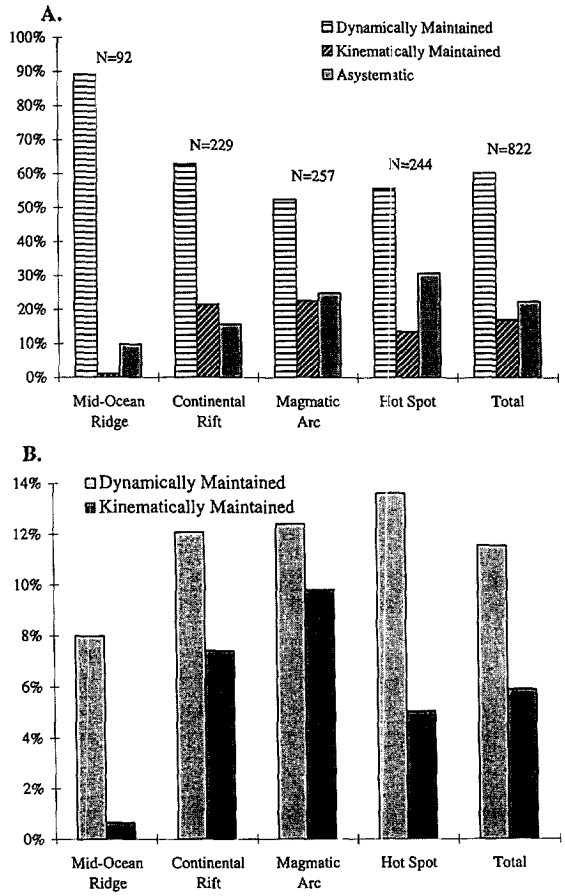

Fig. 12. (A) Relative proportions of dynamically maintained and kinematically maintained hot springs based on mechanical interpretation of the different structural settings. (B) Percentage of hydrothermally active dynamically maintained and kinematically maintained areas normalized to the total abundance of each mechanical designation.

In the following sections, we propose a model for the concurrent evolution of hydrothermal systems and fault zones that integrates the results of our survey and our interpretations based on fault mechanics. We discuss how fault zone development (modeled after Martel and Pollard, 1989; Martel, 1990) may be reflected in the distribution, character, and evolution of hydrothermal outflow sites and hydrothermal deposits. We consider how fault growth and linkage may result in changes in fracture permeability and hydrothermal flow systematics, and lead to changes in the behavior of individual hot springs. Finally, we explore the effects of hydrothermal fluids and mineralization on faulting.

4.2. Fault zone evolution reflected in hydrothermal deposits

Ore bodies, extensively altered and fractured stockworks, and other forms of intense hydrothermal alteration and deposition are found most commonly at fault intersections and in extensional duplexes or releasing bends (Kerrich, 1986; Sibson, 1987; Henley and Adams, 1992; Arribas, 1995). In contrast, thin veneers of hot spring deposits and minor hydrothermal alteration are commonly found along faults (Hulen, 1978; Sibbett and Nielson, 1980; Curewitz, unpubl. data). When we combine these observations with the results of our survey, a possible explanation emerges for the relative abundance of active hot springs in different sites, the distribution of permeability in fault zones, and the distribution and character hydrothermal deposits.

Stresses, especially tensile stresses, should be concentrated in the tip-line area of a fault, where they are capable of opening fractures and focusing fluid flow. However, as the fault propagates through the crust, its tip line moves. Individual tip-line hot springs will die out behind the migrating breakdown region as the elevated stresses that maintain fracture permeability migrate with the tip-line area. New hot springs will form at the leading edge of the tip line as the breakdown region migrates, and hot springs that are left behind will cease activity as hydrothermal mineralization clogs the permeable pathways. Lengthening of the fault and propagation of the tip-line area will leave behind a string of hydrother-

mal deposits adjacent to the fault (Fig. 13), similar to a hot spot track in a lithospheric plate.

It is possible that fault evolution history is recorded in the hydrothermal deposits along a fault zone. As isolated faults propagate toward one another they focus fluid flow at their tips and leave behind a string of hydrothermal deposits along the fault trace (Fig. 14A). As fault tips approach one another, their breakdown regions merge, enlarge, and are pinned at one point (Fig. 14B). Hydrothermal activity will then be focused in the area between the two fault tips by the opposing action of the interacting faults (Fig. 14C). Finally, the faults may link and the hydrothermal outflow sites may localize to a single fault intersection or fault bend (Fig. 14D) which is controlled by slip on any of the faults that have linked to form the fault zone.

4.3. Evolution of individual hot springs

Fluid-flow rates and periodicity in geyser/hot spring systems are dependent on several variables including the height of the water table, the temperature of the heat source, and the size and shape of the permeable conduit (Ingebritsen and Rojstaczer, 1993). Narrow, highly fractured conduits with high permeability relative to the surrounding rock promote periodic, explosive, geysering behavior, while wider fractured conduits result in slow flow. As the fractured conduit continues to widen, flow eventually ceases altogether. We expect that fault propagation will induce such changes in fracture density, permeability, and the width of the fractured conduit.

For example, as a fault propagates into a section of crust, there will be an initial sharp rise in fracture

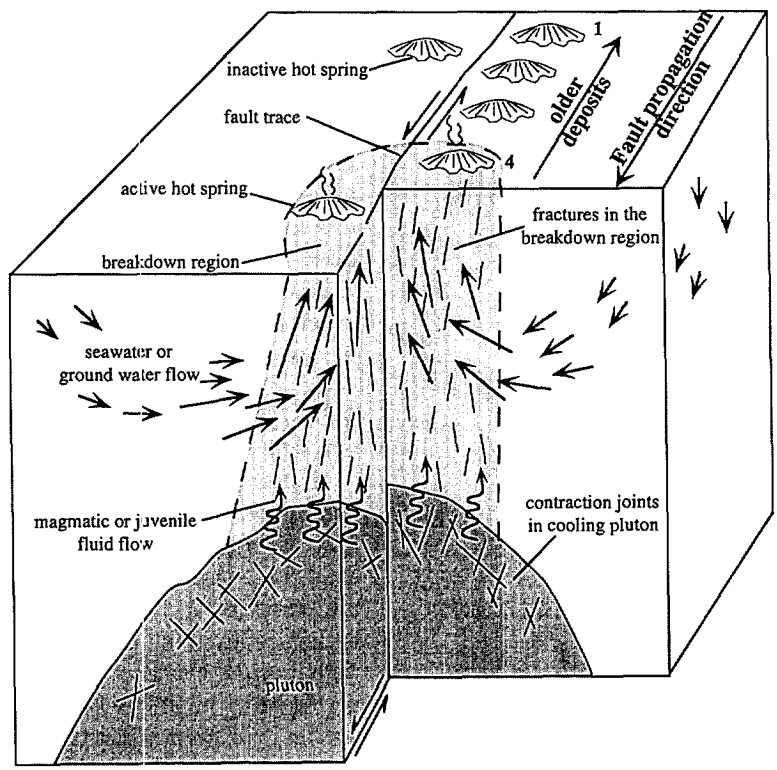

Fig. 13. Schematic diagram showing the different components of hydrothermal systems as they might occur at the tip of a left-lateral strike-slip fault near a young pluton. Meteoric water travels through the crust and is heated by the pluton. Small amounts of magmatic fluids may be released by fracturing at the pluton margin during cooling. These fluids are subsequently focused and channeled by the fractures surrounding the tip-line of the propagating fault and reach the surface as hot springs. The oldest hot spring deposits are found at (*1*) farthest away from the propagating tip of the fault. The youngest deposits are found at (*4*) nearest the propagating tip.

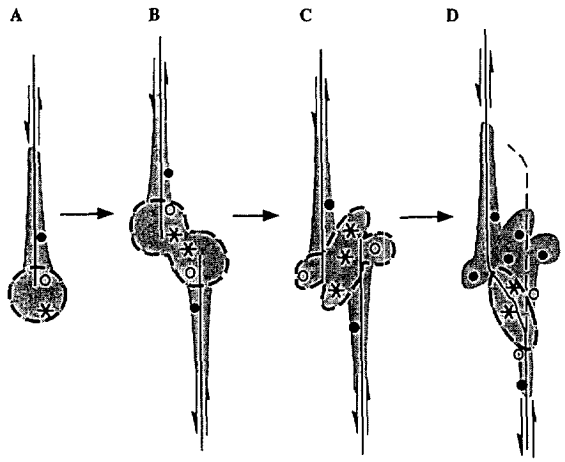

Fig. 14. Schematic map views of the evolutionary steps during maturation of a fault/hydrothermal system. Symbols as follows: * = dynamically maintained high temperature, geyser; ○ = dynamically maintained, lower temperature, steady flow; ● = kinematically maintained, cold spring, steady flow. The breakdown region is delimited by a dashed line, areas of hydrothermal alteration and deposits are shaded. (A) An isolated fault has associated dynamically maintained and kinematically maintained hot springs. (B) The isolated fault begins to approach another fault, and the faults begin to interact. (C) The two faults continue to propagate and interact in an expanding region. (D) The two faults link and behave mechanically as a single fault with a fault bend where stress is concentrated. Slip ceases on the abandoned (dashed) branch of the right-hand fault. The spatial arrangement, temperature, and behavior of hot springs, and the different patterns of hydrothermal deposition are a reflection of the change in size and shape of the highly permeable area created and maintained by stress increases in the breakdown region. Age and morphology of hot spring deposits reflect the evolution and eventual linkage of the faults at the surface to form a continuous fault zone.

density in the small area that is on the boundaries of the advancing breakdown region. This will promote the formation of explosive geysers. As the fault propagates and the breakdown region migrates with it through the crust, the width of the fractured conduit will increase and permeability contrasts will decrease. This may result in the initiation of new of geysers in the new fault tip area, and the onset of steady flow in hot springs along the fault. Eventually, with continued fault propagation, what were once tip-line hot springs will be entirely outside the breakdown region, and will cease activity as hydrothermal mineral precipitation clogs fractures.

Alternatively, hot springs in an interaction area or at a fault intersection could be rejuvenated by reopening of fractures. In this case an individual hot spring could cease activity as mineral precipitation clogs the permeable pathways that supply it. Subsequent slip on any of the interacting or intersecting faults may promote fracturing, and the hot spring could resume activity as conduits for fluid flow are reopened. Thus individual deposits may have a 'stratigraphy' or accretionary history the reflects the history of fault movement in that area.

4.4. Effects of hydrothermal processes on faulting

The controls that faults exert on hydrothermal systems have been discussed above. Conversely, it is likely that hydrothermal systems exert significant influence on faulting. Hot (> 150–300°C) hydrothermal fluids (Carter et al., 1990; Hannington et al., 1995) scavenge soluble minerals and decrease the strength of rocks. These same fluids can precipitate hydrous minerals and other amorphous solids that may be significantly weaker than pre-existing non-fractured rocks (Elders et al., 1979, 1984; Bishop and Bird, 1987). In addition, precipitation of these minerals in fractures and along faults can clog permeable pathways and restrict fluid flow, thereby increasing pore-fluid pressures (Phillips, 1972; Sibson, 1981). Increased pore-fluid pressures decrease normal stresses in a fault zone or tip-line area, and could promote fault slip or propagation (Bartley and Glazner, 1985; Axen, 1992).

Therefore, there may be feedback between faulting and hydrothermal activity. Fault propagation and interaction create and maintain permeability by concentrating stresses and fracturing the crust. Increased permeability leads to fluid flow and concentrated hydrothermal outflow. Decreased strength, lubrication, and increased pore pressure arise in fault zones as a result of fluid–rock interaction. These effects in turn increase the potential for fault slip or propagation. This relationship between faults and hydrothermal systems highlights the complex interdependency that may result from faulting, associated fine-scale fracturing, and hydrothermal fluid flow.

5. Conclusions

Hot springs are found most commonly in specific structural settings with respect to faults: primarily in fault interaction areas, and somewhat less commonly at fault tip-lines and fault intersections. These are sites of active fracturing where permeable pathways are created and maintained despite clogging by hydrothermal mineral precipitates. As faults propagate, interact, and link, hydrothermal outflow may evolve from scattered, migrating discharge sites at the tips of individual faults, to focused, stable discharge sites located in fault interaction areas or at fault intersections. The distribution and character of hydrothermal deposits along fault zones, as well as changes in the behavior of hot springs near faults may reflect the concurrent evolution of fault zones and hydrothermal systems.

Acknowledgements

Field work funded by GSA grant number 5578-95 and a Sigma Xi grant in aid of research. Many thanks to Dr. Wilfred Elders and Dr. Bruce Marsh for their insightful and constructive manuscript reviews. Additional thanks to R. Lawrence, B. Meurer, J. Lakings, S. Rojstaczer and P. Malin for their input, ideas and enthusiasm for this work.

References

Allen, E.T., Day, A.L., 1935. Hot springs of the Yellowstone National Park. Carnegie Inst. Washington Publ. 466, 525 pp.

Allmendinger, R.W, Gephart, J.W., Marrett, R.A., 1989. Notes on fault slip analysis. In: Allmendinger, R.W., Aydin, A., Engelder, T., Pollard, D.D. (Eds.), Quantitative Interpretation of Joints and Faults. Geol. Soc. Am. Annu. Meet. 1989.

Anders, M.H., Wiltschko, D.V., 1994. Microfracturing, paleostress and the growth of faults. J. Struct. Geol. 16 (6), 795–815.

Anderson, D.N., Axtell, L.H., 1972. Geothermal resources in California. In: Anderson, D.N., Axtell, L.H. (Eds.), Geothermal Overviews of the Western United States. Geothermal Resources Council, pp. 16–52.

Andrews, D.J., 1989. Mechanics of fault Junctions. J. Geophys. Res. 94 (B7), 9389–9397.

Arango, 1970. Preliminary study on the Ruiz hydrothermal project. In: Tongiorgi, E. (Ed.), Proceedings of the United Nations Symposium on the Development and Utilization of Geothermal Resources. Geothermics, Spec. Iss. 2.

Arribas, Jr., A., 1995. Characteristics of high-sulfidation epithermal deposits, and their relation to magmatic fluid. In: Jambor, J.L. (Ed.), Magmas, Fluids, and Ore Deposits. Mineral. Assoc. Can. Short Course Ser. 23, 419–454.

Axen, G.J., 1992. Pore pressure, stress increase, and fault weakening in low-angle normal faulting. J. Geophys. Res. 97, 8979–8991.

Aydin, A., Page, B.M., 1984. Diverse Pliocene–Quaternary tectonics in a transform environment, San Francisco Bay region, California . Geol. Soc. Am. Bull. 95, 1303–1317.

Aydin, A., Reches, Z., 1982. Number and orientation of fault sets in the field and in experiments. Geology 10, 107–112.

Banwell, Valle, 1970. Geothermal Exploration in Mexico. In: Tongiorgi, E. (Ed.), Proceedings of the United Nations Symposium on the Development and Utilization of Geothermal Resources. Geothermics, Spec. Iss. 2.

Barth, T.F.W., 1950. Volcanic Geology, Hot Springs, and Geysers of Iceland. Carnegie Inst. Washington Publ. 587.

Bartley, J.M., Glazner, A.F., 1985. Hydrothermal systems and Tertiary low-angle normal faulting in the southwestern United States. Geology 13, 562–564.

Barton, C.A., Zoback, M.D., Moos, D., 1995. Fluid flow along potentially active faults in crystalline rock. Geology 23 (8), 683–686.

Bishop, B.P., Bird, D.K., 1987. Variation in sericite compositions from fracture zones within the Coso Hot Springs geothermal system. Geochim. Cosmochim. Acta 51, 1245–1256.

Boullier, A.-M., Charoy, B., Pollard, P.J., 1994. Fluctuation in porosity and fluid pressure during hydrothermal events: textural evidence in the Emuford District, Australia . J. Struct. Geol. 16 (10), 1417–1429.

Boyer, S.E., Elliott, D., 1982. Thrust systems . Am. Assoc. Pet. Geol. Bull. 66, 1196–1230.

Brace, W.F., 1980. Permeability of crystalline and argillaceous rocks. Int. J. Mech. Min. Sci. Geomech Abstr. 17, 241–251.

Bruhn, R.L., Yonkee, W.A., Parry, W.T., 1990. Structural and fluid-chemical properties of seismogenic normal faults. Tectonophysics 175, 139–157.

Burgmann, R., Pollard, D.D., 1994. Strain accommodation about strike-slip fault discontinuities in granitic rock under brittle-to-ductile conditions. J. Struct. Geol. 16, 1655–1674.

Carter, N.L., Kronenberg, A.K., Ross, J.V., Wiltschko, D.V., 1990. Control of fluids on deformation of rocks. In: Knipe, R.J., Rutter, E.H. (Eds.), Deformation Mechanisms, Rheology and Tectonics. Geol. Soc. Spec. Publ. 54, 1–13.

Cioni, R., Fanelli, G., Giudi, M., 1992. Lake Bogoria Hot Springs (Kenya): geochemical features and geothermal implications. J. Volcanol. Geotherm. Res. 50, 231–246.

Cormy, 1970. Prospection Geothermique aux Antilles Francais. In: Tongiorgi, E. (Ed.), Proceedings of the United Nations Symposium on the Development and Utilization of Geothermal Resources. Geothermics, Spec. Iss. 2.

Cowie, P.A., Scholz, C.H., 1992. Physical explanation for the displacement–length relationship of faults using a post-yield fracture mechanics model. J. Struct. Geol. 14, 1133–1148.

Dawers, N.H., Anders, M.H., Scholz, C.H., 1993. Growth of normal faults: Displacement–length scaling. Geology 21, 1107–1110.

Delaney, J.R., Robigou, V., Mcduff, R.E., Tivey, M., 1992. Geology of a vigorous hydrothermal system on the Endeavour segment, Juan de Fuca Ridge. J. Geophys. Res. 97, 19663–19682.

Du, Y., Aydin, A., 1995. Shear fracture patterns and connectivity at geometric complexities along strike-slip faults. J. Geophys. Res. 100, 18093–18102.

Ebinger, C.J., Deino, A.L., Tesha, A.L., Becker, T., Ring, U., 1993. Tectonic controls on rift basin morphology: Evolution of the Northern Malawi (Nyasa) rift. J. Geophys. Res. 98, 17821–17836.

Elders, W.A., Hoagland, J.R., McDowell, S.D., Cobo, J.M., 1979. Hydrothermal mineral zones in the geothermal reservoir of Cerro Prieto. Geothermics 8, 201–209.

Elders, W.A., Bird, D.K., Williams, A.E., Schiffman, P., 1984. Hydrothermal flow regime and magmatic heat source of the Cerro Prieto geothermal system, Baja California, Mexico . Geothermics 13, 27–47.

Embley, R.W., Chadwick, W.W., 1994. Volcanic and hydrothermal processes associated with a recent phase of seafloor spreading at the northern Cleft segment: Juan de Fuca Ridge. J. Geophys. Res. 99, 4741–4760.

Embley, R.W., Chadwick, W.W., Jonasson, I.R., Butterfield, D.A., Baker, E.T., 1995. Initial results of the rapid response to the 1993 CoAxial event: Relationships between hydrothermal and volcanic processes. Geophys. Res. Lett. 22 (2), 143–146.

Foulger, G.R., 1988. Hengill triple junction, southwest Iceland: Anomalous earthquake focal mechanisms and implications for process within the geothermal reservoir and at accretionary plate boundaries. J. Geophys. Res. 93, 13507–13523.

Fournier, R.O., 1989. Geochemistry and dynamics of the Yellowstone National Park hydrothermal system. Annu. Rev. Earth Planet. Sci. 17, 13–53.

Gente, P., Mevel, C., Auzende, J.M., Karson, J.A., Fouquet, Y., 1991. An example of a recent accretion on the Mid-Atlantic Ridge: The Snake Pit neovolcanic ridge (MARK area, 23°22′N). Tectonophysics 190, 1–29.

Grimaud, P., Richert, J.-P., Rolet, J., Tiercelin, J.-J., Xavier, J.-P., Morley, C.K., Coussement, C., Karanja, S.W., Renaut, R.W., Guerin, G., Le Turdu, C., Michel-Noel, G., 1994. Fault geometry and extension mechanisms in the Central Kenya Rift, East Africa. A 3D remote sensing approach. Elf Acquitaine Productions, Boussens, France, pp. 59–92.

Grindley, 1970. Surface structures and relation to steam production in the Broadlands geothermal field, New Zealand. In: Tongiorgi, E. (Ed.), Proceedings of the United Nations Symposium on the Development and Utilization of Geothermal Resources. Geothermics, Spec. Iss. 2.

Hannington, M.D., Jonasson, I.R., Herzig, P.M., Petersen, S., 1995. Physical and chemical processes of seafloor mineralization at mid-ocean ridges. In: Humphris, S.E., Zierenberg, R.A., Mullineaux, L.S., Thomson, R.E. (Eds.), Seafloor Hydrothermal Systems: Physical, Chemical, Biological, and Geological Interactions. AGU Geophys. Monogr. 91, 115–157.

Henley, R.W., Adams, D.P.M., 1992. Strike-slip fault reactivation as a control on epithermal vein-style gold mineralization. Geology 20, 443–446.

Henley, R.W., Brown, K.L., 1985. A practical guide to the thermodynamics of geothermal fluids and hydrothermal ore deposits. In: Berger, B.R., Bethke, P.M. (Eds.), Geology and Geochemistry of Epithermal Systems. Rev. Econ. Geol. 2, 25–43.

Henry, C.D., 1979. Geologic setting and geochemistry of thermal water and geothermal assessment, Trans-Pecos Texas. Bur. Econ. Geol. Rep. Invest. 96, 1–44.

Hewitt, W.P., Stowe, C.H., Stromberg, R.R., 1972. Utah's geothermal resources. Location, potential, and administrative agencies. In: Anderson, D.N., Axtell, L.H. (Eds.), Geothermal Overviews of the Western United States. Geothermal Resources Council, pp. 147–160.

Hulen, J.B., 1978. Geology and alteration of the Coso geothermal area, Inyo County, California. U.S. Dep. Energy Rep. N. IDO/78-1701.b.4.1, 41 pp.

Ingebritsen, S.E., Rojstaczer, S.A., 1993. Controls on geyser periodicity. Science 262, 889–892.

Isida, M., 1976. Elastic analysis of cracks and stress intensity factors. In: Baifuukan (Ed.), Fracture Mechanics and Strength of Material II. pp. 193–201.

Kappel, E.S., Franklin, J.M., 1989. Relationships between geologic development of ridge crests and sulfide deposits in the northeast Pacific Ocean. Econ. Geol. 84, 485–505.

Karson, J.A., Rona, P.A., 1990. Block-tilting, transfer faults, and structural control of magmatic and hydrothermal processes in the TAG area, Mid-Atlantic Ridge 26° North. Geol. Soc. Am. Bull. 102, 1635–1645.

Kelley, D.S., Gillis, K.M., Thompson, G., 1993. Fluid evolution in submarine magma-hydrothermal systems at the Mid-Atlantic Ridge. J. Geophys. Res. 98, 19576–19579.

Kerrich, R., 1986. Fluid infiltration into Fault Zones: Chemical, isotopic, and Mechanical effects. Pageoph 124 (1–2), 225–268.

King, G.C.P., Stein, R.S., Lin, J., 1994. Static stress changes and the triggering of earthquakes. Bull. Seismol. Soc. Am. 84 (3), 935–953.

Lachenbruch, A.H., 1980. Frictional heating, fluid pressure, and the resistance to fault motion. J. Geophys. Res. 85, 6097–6112.

Lalou, C., Reyss, J.-L., Brichet, E., Arnold, M., Thompson, G., Fouquet, Y., Rona, P.A., 1993. New age data for Mid-Atlantic Ridge hydrothermal sites: TAG and Snakepit chronology revisited. J. Geophys. Res. 98, 9705–9713.

Link, P.K., Kuntz, M.A., Platt, L.B. (Eds.), 1992. Regional Geology of Eastern Idaho and Western Wyoming. Geol. Soc. Am. Boulder, CO, 312 pp.

Martel, S.J., 1990. Formation of compound strike-slip fault zones, Mount Abbot quadrangle, California . J. Struct. Geol. 12, 869–882.

Martel, S.J., Petersen, J.E., 1991. Interdisciplinary characterization of fracture systems at the US/BK Site, Grimsel Laboratory, Switzerland. Int. J. Rock Mech. Min. Sci., Geomech. Abstr. 28 (4), 295–323.

Martel, S.J., Pollard, D.D., 1989. Mechanics of slip and fracture along small faults and simple strike-slip fault zones in granitic rock. J. Geophys. Res. 94, 9417–9428.

McConachy, T.F., 1984. The geological form and setting of a hydrothermal ventfield at 10°56′N, East Pacific Rise: A de-

tailed study using Angus and Alvin. Woods Hole Oceanogr. Inst., Course-work Pap.

McKenzie, D., 1978. Some remarks on the development of sedimentary basins. Earth Planet. Sci. Lett. 40, 25–32.

Mottl, M.J., 1983. Metabasalts, axial hot springs, and the structure of hydrothermal systems at mid-ocean ridges. GSA Bull. 94, 161–180.

N. Z. Dep. Sci. Ind. Res., 1963. Waiotapu Geothermal Field. Bull. 155, 141 pp.

Norton, D., Knapp, R., 1977. Transport phenomena in hydrothermal systems: The nature of porosity. Am. J. Sci. 22, 913–936.

Peacock, D.C.P., 1991. Displacements and segment linkage in strike-slip fault zones. J. Struct. Geol. 13, 1025–1035.

Peacock, D.C.P., Sanderson, D.J., 1994. Geometry and development of relay ramps in normal fault systems. AAPG Bull. 8 (2), 147–165.

Peacock, D.C.P., Sanderson, D.J., 1995. Pull-aparts, shear fractures and pressure solution. Tectonophysics 241, 1–13.

Person, M., Raffensperger, J.P., Ge, S., Garvin, G., 1996. Basin-scale hydrogeologic modeling. Rev. Geophys. 34 (1), 61–87.

Phillips, W.J., 1972. Hydraulic fracturing and mineralization. J. Geol. Soc. London 128, 337–359.

Pollard, D.D., Aydin, A., 1988. Progress in understanding jointing over the past century. Geol. Soc. Am. Bull. 100, 1181–1204.

Puente, C.I., De La Pena, A.L., 1979. Geology of the Cerro Prieto geothermal field. Geothermics 8, 155–175.

Rimstidt, J.D., Barnes, H.L., 1980. The kinetics of silica–water reactions. Geochim. Cosmochim. Acta 44, 1683–1699.

Robigou, V., Delaney, J.R., Stakes, D.R., 1993. Large massive sulfide deposits in a newly discovered active hydrothermal system, the High-Rise Field, Endeavour Segment, Juan de Fuca Ridge . Geophys. Res. Lett. 20 (17), 1887–1890.

Sato, K., 1970. The present state of geothermal energy in Japan, In: E. Tongiorgi (Ed.), Proceedings of the U.N. Symposium on the Development and Utilization of Geothermal Resources. Geothermics Spec. Iss. 2, 155–185.

Scholz, C.H., 1980. Shear heating and the state of stress on faults. J. Geophys. Res. 85, 6174–6184.

Scholz, C.H., 1990. The Mechanics of Earthquakes and Faulting. Cambridge Univ. Press, New York, NY, 439 pp.

Scholz, C.H., Anders, M.H., 1994. The permeability of faults, In: Hickman, Sibson, Bruhn (Eds.), The Mechanical Involvement of Fluids in Faulting. USGS Red Book LXIII, O.F. Rep. 94-228, 247–253.

Scholz, C.H., Dawers, N.H., Yu, J.Z., Anders, M.H., Cowie, P.A., 1993. Fault growth and fault scaling laws: Preliminary results. J. Geophys. Res. 98, 21951–21961.

Segall, P., Pollard, D.D., 1980. Mechanics of discontinuous faults. J. Geophys. Res. 85, 4337–4350.

Sibbett, B.S., Nielson, D.L., 1980. Geology of the Central Mineral Mountains, Beaver County, Utah. Dep. Energy, Div. Geotherm. Energy, Rep. DOE/ET/28392-40, 42 pp.

Sibson, R.H., 1981. Controls on low-stress hydro-fracture dilatancy in thrust, wrench and normal fault terrains. Nature 289, 665–667.

Sibson, R.H., 1985. Stopping of earthquake ruptures at dilational fault jogs. Nature 316, 248–251.

Sibson, R.H., 1987. Earthquake rupturing as a mineralizing agent in hydrothermal systems. Geology 15, 701–704.

Stein, R.S., Barka, A.A., Dieterich, J.H., 1996. Progressive failure on the North Anatolian fault since 1939 by earthquake stress triggering. Geophys. J. Int.

Ten-Dam and Khrebtov, 1970. The Menderes Massif geothermal prospect, Turkey, In: Tongiorgi, E. (Ed.), Proceedings of the United Nations Symposium on the Development and Utilization of Geothermal Resources. Geothermics, Spec. Iss. 2.

Tiercelin, J.-J., Thouin, C., Kalala, T., Mondeguer, A., 1989. Discovery of sublacustrine hydrothermal activity and associated massive sulfides and hydrocarbons in the north Tanganyika trough East African Rift . Geology 17, 1053–1056.

Tole, M.P., 1990. Present day ore deposition in the geothermal systems of Kenya—I. The Mwananyamala Hot Springs, northeast of Jombo Hill, Coast Province. Geothermics 19, 233.

White, D.E., Thompson, G.A., Sandberg, C.H., 1964. Rocks, structure, and geologic history of Steamboat Springs Thermal Area, Washoe County Nevada. USGS Prof. Pap. 458-B, 63 pp.

Wohletz, K., Heiken, G., 1992. Volcanology and Geothermal Energy. Univ. California Press, Berkeley and Los Angeles, CA, 432 pp.

Yamasaki, 1970. Geology of hydrothermal alterations of Otake geothermal area, Japan, In: Tongiorgi, E. (Ed.), Proceedings of the United Nations Symposium on the Development and Utilization of Geothermal Resources. Geothermics, Spec. Iss. 2.